

Influence of water models on water movement through AQP1

Miguel A. Gonzalez,^{*,†} Alberto Zaragoza,[‡] Charlotte I. Lynch,[¶] Mark S.P.
Sansom,[¶] and Chantal Valeriani[§]

[†]*Universidad Rey Juan Carlos, ESCET, 28933, Mostoles-Madrid, Spain*

[‡]*Department of Chemistry, The University of Utah, Salt Lake City, Utah 84112-0850, USA*

[¶]*University of Oxford, Department of Biochemistry, South Parks Road, OX1 3QU, Oxford,
UK*

[§]*Universidad Complutense de Madrid, Facultad de Ciencias Físicas, Departamento de
Estructura de la Materia, Física Térmica y Electrónica, 28040, Madrid, Spain*

E-mail: miguelangel.gonzalez@urjc.es

Phone: +34 91 488 82 80

Abstract

Water diffusion through membrane proteins is a key aspect of cellular function. Essential processes of cellular metabolism are driven by osmotic pressure, which depends on water channels. Membrane proteins such as aquaporins (AQPs) are responsible for enabling water transport through the cell membrane. AQPs are highly selective, allowing only water and relatively small polar molecules to cross the membrane. Experimentally, estimation of water flux through membrane proteins is still a challenge, and hence accurate simulations of water transport are of particular importance. We present a numerical study of water diffusion through AQP1 comparing three water models: TIP3P, OPC and TIP4P/2005. Bulk diffusion, diffusion permeability and osmotic permeability are computed and compared among all models. The results show that there are significant differences between TIP3P (a particularly widespread model for simulations of biological systems), and the more recently developed TIP4P/2005 and OPC models. We demonstrate that OPC and TIP4P/2005 reproduce protein-water interactions and dynamics in excellent agreement with experimental data. From this study, we find that the choice of the water model has a significant effect on the computed water dynamics as well as its molecular behaviour within a biological nanopore.

Introduction

Water is the most abundant molecule in cells. Even though water is able to diffuse slowly through a lipid bilayer, for essential physiological processes a high water flux is required. This can be achieved making use of protein membranes such as aquaporins (AQPs) which allow for a high selectivity for water transport across biological membranes.^{1,2} AQPs are located in several cells found in the brain, kidneys, skin, blood vessels, liver and connective tissue.^{3,4} The lack of functionality of such cells might induce several diseases, such as glaucoma, brain edema or congestive heart failure.^{3,5,6} Although evidence of the existence of water channels had been reported several years earlier, the aquaporin structure was not described until

1992.⁷ All members of the AQP family are small (~ 30 kDa) intrinsic membrane proteins with a strongly hydrophobic character, and consist of four monomers. Each monomer is a functional water channel having a hourglass shape⁸ with an amphiphilic interior and a selectivity filter. The primary sequence of those proteins shows six trans-membrane helices (I-VI) linked by five loops. The water flux inside the channel depends on an asparagine-proline-alanine (NPA) motif, found in two loops located approximately in the middle of the membrane protein channel. The interaction between these motifs not only confers a particular shape to the channel but it is also responsible for the orientation of water molecules inside the channel. In combination with the NPA motif, water transport is also modulated by the aromatic/arginine selectivity filter which is situated next to the extracellular exit/entrance of the channel.^{9,10} The topology of the pore is extremely important as it enables selected small polar molecules to cross the membrane (e.g. H_2O , NH_3 , glycerol) whilst preventing the passage of others (e.g. ions and larger molecules). Based on its permeability, AQPs can be classified in two subfamilies: classical aquaporins (permeable to water) and aquaglyceroporins (permeable to both water and glycerol).

AQP1 is a classical aquaporin with a high water permeability as described in detail in Ref.¹¹ and confirmed in several numerical studies.^{9,10,12-15} Numerous molecular dynamics studies have been conducted on the water permeation mechanism through aquaporins.^{11,12,16-24} As discussed by Ozu *et al.*,²⁵ many AQP simulations have been carried out using different force fields (GROMOS or CHARMM) for the protein and the standard older TIP3P or SPC water models. De Groot and Grubmüller¹⁶ demonstrated that proton translocation across AQPs was prevented by an electrostatic barrier. However Jensen *et al.*,²² using a different force field to simulate AQP and water (TIP3P), concluded that the proton induced an interruption of the hydrogen bond chain network built into the channel, forbidding the proton to cross the pore. Thus, it is reasonable to suggest that models of water transport might be affected by the force field used to simulate water molecules.

When dealing with pure water, both Vega *et al.*²⁶ and Onufriev *et al.*²⁷ carried out

a detailed comparison between experimental and numerical values of thermodynamic and dynamic properties, simulating water by means of several interaction potentials. Even though they clearly demonstrated that TIP3P was not one of the best performing potentials for pure water, TIP3P remains a widely used water model in biomolecular simulations, in combination with CHARMM (the most widely used protein force field). With this in mind, we propose to study the molecular mechanism of water transport of AQP1 (1H6I code PDB)¹² simulated with CHARMM36m,²⁸ in combination with the TIP3P, OPC and TIP4P/2005 water models. Even though the latter two water models are less frequently used in biomolecular simulations, they are known to give very reliable thermodynamic and dynamic properties for bulk water. To our knowledge, TIP4P/2005 has been already implemented with the AMBER ff03w²⁹ force field as a default water model but has not been employed in simulations of AQP, where the microscopic behaviour of water clearly plays a vital role. In this article, we have studied several properties of human AQP1 (water diffusion across the pore, diffusion permeability and osmotic permeability) taking into account the molecular mechanism characteristic of AQP. The results obtained allow us to compare the water models and to select the best one depending on its performance in the presence of the protein channel.

Theory and Methods

Simulation details

We have carried out molecular dynamics simulations for AQP1 embedded in a palmitoyl-oleoylphosphatidylcholine (POPC) bilayer membrane using the GROMACS 2016.4 software package.³⁰ Human AQP1 (1H6I code PDB)¹² is simulated via the CHARMM36m force field,²⁸ whilst the water molecules are simulated using TIP3P,³¹ OPC,³² and TIP4P/2005³³ potentials. Considering the three models of water, we have set up three initial configurations with the AQP1 tetramer embedded in a lipid bilayer of 209 POPC molecules and solvated with approx. 20000 water molecules. In order to prepare a neutral configuration, we have

added 4 Cl^- ions. Each AQP1-water system was simulated for 100 ns, and simulations were repeated four times with different random initial velocities. We set a time step of 1 fs keeping the temperature constant at 298 K using a velocity rescale thermostat³⁴ with a relaxation time set to 0.67 ps. The Parrinello-Rahman barostat³⁵ was applied to maintain the pressure constant at 1 bar using a 2.57 ps relaxation time. When dealing with water, the Lennard-Jones (LJ) potential was truncated at 1.2 nm, adding standard long-range corrections to the LJ energy. Ewald sums³⁶ were considered to compute long-range electrostatic forces with a real space cut-off at 1.2 nm. In order to compare the behaviour of the three water models and their interactions with AQP1, we have selected the most relevant properties that allow us to establish the influence of water potentials on water dynamics through protein channels.

Diffusion, diffusion permeability, rate of water molecules and average dipole moment across the channel

Water diffusion through a cell membrane is considered as a subdiffusive process.³⁷⁻⁴¹ Yamamoto *et al.*⁴² demonstrated that the water subdiffusion near a lipid membrane is due to two mechanisms. On the one hand, there is a divergent mean trapping time induced by the lipid-water interaction which can be described by a continuous-time random walk. On the other hand, the viscoelasticity of the lipid membrane induces a long-time correlated noise described by fractional Brownian motion. In order to compute water diffusion, we distinguished four regions depending on the distance (d) between the lipid headgroup and the position of the water molecule. As in Ref. 40, the criteria applied to create those regions are the following: we identify a 1) bulk region whenever $d > 0.6$ nm, an 2) interface region whenever $0.3 \text{ nm} < d < 0.6 \text{ nm}$, a 3) contact region whenever $d < 0.3 \text{ nm}$) and an 4) AQP region defined as the region inside the lipid headgroups (corresponding to waters in the pore). The long time diffusion coefficient (D) is then computed using Einstein's relation based on

the water mean square displacement:

$$D = \frac{\langle |r(t_0 + t) - r(t_0)|^2 \rangle}{2 \cdot dim \cdot t} \quad (1)$$

where $r(t)$ is the position of the water molecule centre of mass, t is the time, and dim the dimension that depends on the geometry of the system where the molecules are moving through, with $dim = 1$ for 1D geometries such as carbon nanotubes CNT or AQP1 and $dim = 3$ for bulk.⁴³

Another approach to calculate water diffusion inside the protein channel (AQP region) is based on a single-water molecule column.⁴⁴ In this case, water diffusion (D_z) is computed according to the relation:⁴⁵

$$D_z = \frac{k_0 z^2}{2} = \frac{z^2 p_f}{2\nu_w} \quad (2)$$

where k_0 , z , p_f and ν_w are the rate of water molecules across the channel, the average distance between two water molecules inside the channel, the osmotic permeability (see below for more details) and the volume of a single molecule, respectively.

Water permeability can be divided into osmotic permeability (p_f) and diffusion permeability (p_d) depending on the system's conditions. Osmotic pressure drives the movement of water molecules through the membrane protein when there is a solute gradient across the membrane. Hence in these conditions water permeability would be given by the osmotic permeability of the system. Following Ref.,⁴⁶ osmotic permeability is defined as the proportionality constant between the net water flux (j_w) across the protein channel and the solute concentration difference (ΔC_s),

$$j_w = p_f \Delta C_s. \quad (3)$$

Taking into account the rate of water molecules across the membrane protein, k_0 , the osmotic permeability is also defined as

$$p_f = \nu_w k_0. \quad (4)$$

At equilibrium and in the absence of solute or solute gradient, there is still a net water flux through the channel that could be attributed to diffusion of water molecules due to temperature. Thus, the diffusion permeability, p_d , allows us to study the water flux across the protein under these conditions:

$$j_{tr} = p_d \Delta C_{tr} \tag{5}$$

where ΔC_{tr} corresponds to the difference in the tracer's concentration between the two sides of the membrane and j_{tr} is the net tracer's flux (where a tracer is defined as a labelled water molecule that can be distinguished from similar molecules, *i.e.* a molecule of heavy water is a tracer for water). At equilibrium, the rate of water molecules crossing the channel is computed by q_0 , which is related to p_d via

$$p_d = (V_w/N_a)q_0 = \nu_w q_0. \tag{6}$$

Molecular simulations become an essential tool to compute p_d as they allow us to label individual water molecules and therefore distinguish them from one another. Both properties, p_d and p_f , are proportional to the number of water molecules, N , taking part to the translocation following the continuous-time random-walk process⁴⁴ based on Ref.⁴⁷ For AQP1, Zhu *et al.*⁴⁶ presented a value for $p_f/p_d = N + 1 = 11.9$. This is in good agreement to the experimental value of $p_f/p_d = 13.2$.⁴⁸ However, these values are higher than the average number of molecules inside the protein channel, since there are molecules of water outside the channel that participate in the transport across the membrane.

In order to compute the flux in Eq. 5 we need to compute p_d and ΔC_{tr} . The latter is computed by simple counting whereas the former is computed via Eq. 6. To compute q_0 in Eq. 6 we count the number of water molecules that cross the membrane through the AQP1. Thus, we define the centre of the protein and a typical distance from which a molecule is considered to be outside the channel. The channel centre is identified in the following way:

two nitrogen atoms inside the channel are bound to water via hydrogen bonds and their orientation is essential to describe the AQP1 permeability. Thus, we compute the channel centre as the average of these nitrogen atom positions. The channel length is set at 1.5 nm from the centre.

Water molecules in bulk are characterised by an average dipole moment equal to zero. However, in nano-confined structures such as a CNT⁴³ or membrane channels,¹¹ there is a particular orientation of the molecules due to the hydrogen bond network. Thus, the dipole moment is an important parameter to study the molecular orientations inside the channel, both artificial and natural. In our work, we have computed the water dipole moment μ according to $\vec{\mu} = \sum_i q_i \vec{r}_i$, where q_i and r_i are the charge and the position vector for molecule i , respectively. We focus on the z component of $\vec{\mu}$, since in our simulations the orientation of the water molecule inside the channels is mainly projected onto this axis. Hence, we calculate the average dipole moment of slabs, having a thickness of 0.025 nm, across the z axis to compare the molecular orientation between the channel and molecules.

Results

Water molecule orientations inside AQP1

As suggested in Ref.,¹¹ water molecules arrange inside the channel forming a single-molecule chain with a specific orientation. In our work we demonstrate that this mechanism is reproduced by the three water models. As shown in Fig. 1, the water molecule orientation can be illustrated by computing the average of the z component of the dipole moment inside the channel. Although there is a dynamic transport across the channel, it is possible to distinguish the positions of water molecules, described by the slightly ragged shape of the water dipole moment inside the protein. These results demonstrate that there are two stable orientations inside the channel as described by Ref.¹¹

There are no major differences between the dipole moment profiles for the three water

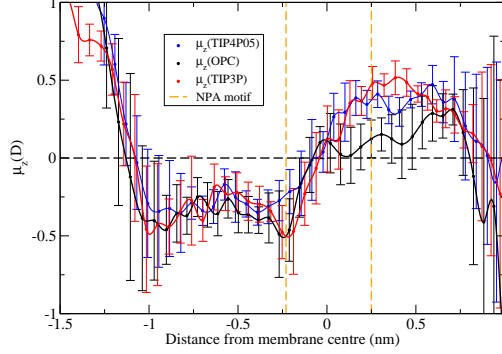


Figure 1: z component of the average dipole moment μ_z for the three water models. The red line is for TIP3P, the blue line for TIP4P/2005, and the black line for OPC. Error bars have been added taking into account the standard deviation of μ_z . The vertical dashed lines indicate the approximate locations of the Asn residue of the NPA motifs. Note that the centre of the bilayer is at $z = 0$ nm, and the pore runs from approximately $z = -1$ to $+0.8$ nm.

models, although the degree of water dipole orientation is less for the OPC model in the second (i.e. $z > 0$) half of the pore than for the other two water models.

Water molecule diffusion through the protein channel

As in Ref. 40, we identify interfacial, pore and contact regions, depending on the position of the water molecule with respect to the bilayer and the AQP1 pore. To compute the water diffusion constant (D) we use Eq. 1 with $dim = 3$ for the bulk (D_{bulk}), interface (D_{inter}), and contact ($D_{contact}$) regions, and $dim = 1$ for the AQP (D_{AQP}) region (AQP1 being almost cylindrical). Moreover, we compare the value of the diffusion computed in the bulk region at $d > 0.6$ nm (D_{bulk}) to the one computed for each model in bulk (D_{model}), since the presence of the lipid membrane reduces the value of D in nearby regions (even at distances higher than 2 nm⁴²). All mean square displacements (msd) for each region are reported in Fig. 2. Two groups of data could be distinguished for each model (although in the case of TIP3P it is more evident). The bulk, interface and contact regions have similar slopes, while the slope for the AQP region is lower than the rest. The diffusion coefficient (D) values for all water models in bulk and in the various regions are presented in Table 1 (as calculated from

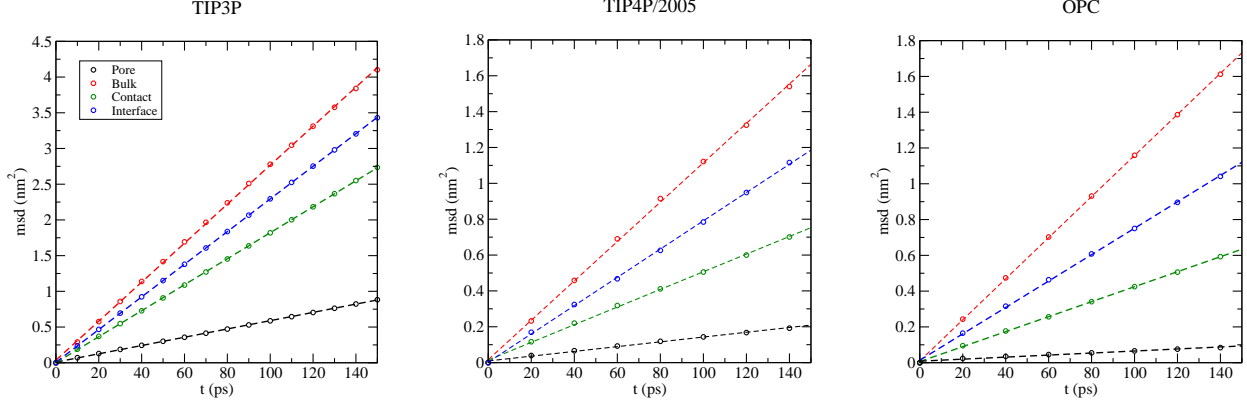


Figure 2: Mean square displacement (nm^2) for TIP3P (left), TIP4P/2005 (centre), and OPC (right). The coloured lines denote the following regions: bulk (red), interface (blue), lipid-water contact region (green), and AQP (black).

the mean square displacement in Fig. 2).

Table 1: Diffusion coefficient values computed using Eq. 1 with $\text{dim} = 3$ in the bulk, interface and contact region, with $\text{dim} = 1$ in the AQP region for TIP3P, TIP4P/2005 and OPC water models. The values in parenthesis are the standard deviations. All diffusion coefficients are expressed in $(\text{cm}^2/\text{s}) 10^{-5}$.

	D_{bulk}	D_{inter}	D_{contact}	D_{PORE}
TIP3P	4.60 (0.01)	3.74 (0.02)	2.93 (0.02)	0.10 (0.01)
TIP4P/2005	1.87 (0.04)	1.24 (0.1)	0.77 (0.04)	0.05 (0.02)
OPC	1.94 (0.04)	1.26 (0.08)	0.72 (0.09)	0.02 (0.02)
Exp.	2.30 ²⁶			0.04 ⁴⁵

The literature values of $D_{\text{literature}}$ at 298K and 1 bar are $5.5 \times 10^{-5} \text{ cm}^2/\text{s}$ ⁴⁹ for TIP3P, $2.06 \times 10^{-5} \text{ cm}^2/\text{s}$ for TIP4P/2005³³ and $2.3 \times 10^{-5} \text{ cm}^2/\text{s}$ ³² for OPC $D_{\text{literature}}$. These data are higher than the D_{bulk} computed from the mean square displacement in our simulations (see Fig. 2), reflecting minor differences in the simulation conditions. However, it is clear that TIP4P/2005 and OPC water models reproduce the experimental water diffusion better than TIP3P. On the one hand, although it is possible to consider TIP3P water subdiffusing as D is compared to $D_{\text{literature}}$, TIP3P overestimates water diffusion in comparison to the experimental data of $2.3 \times 10^{-5} \text{ cm}^2/\text{s}$ in all regions. On the other hand, TIP4P/2005 and OPC show a consistent subdiffusion of water molecules close to the membrane, as expected⁴² both with respect to their $D_{\text{literature}}$ and in comparison to the experimental value. Focusing on

the AQP region, *i.e.* inside the membrane protein, the experimental data of water diffusion is $0.04 \times 10^{-5} \text{ cm}^2/\text{s}$.⁴⁵ TIP3P gives $0.10 \times 10^{-5} \text{ cm}^2/\text{s}$ for D_{PORE} , which is dramatically higher than the experimental value and also higher than the other water models, $0.05 \times 10^{-5} \text{ cm}^2/\text{s}$ and $0.02 \times 10^{-5} \text{ cm}^2/\text{s}$ for TIP4P/2005 and OPC, respectively.

In order to visualise the values of D across the four regions, a diffusion profile has been plotted for each water model, see Fig. 3. This shows the diffusion profiles for the three models by considering only the molecules that have crossed the membrane through the protein channel, as these molecules allow us to compute the water diffusion through the channel.

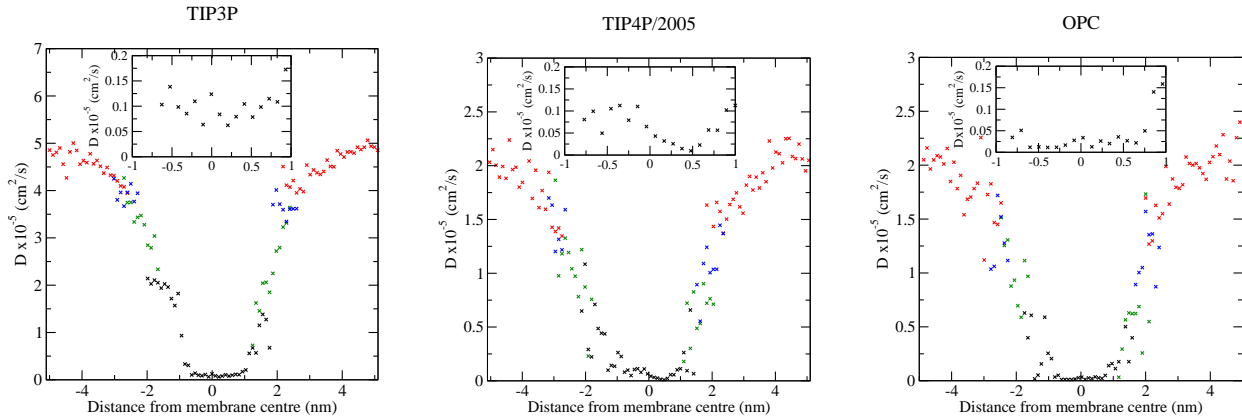


Figure 3: Diffusion profiles for TIP3P (left), TIP4P/2005 (centre), and OPC (right) water models. The profiles have been split into four regions: bulk (red crosses), interface (blue crosses), lipid-water contact (green crosses), and AQP region (black crosses). Note the larger D axis scale for the TIP3P model.

It can be observed that D decreases from the bulk region to the AQP region, starting from a value of D lower than $D_{literature}$. Each region displays a distinct diffusion profile, although there is a slight overlap between regions. This is due to the criteria used to define the regions, *i.e.* an average of the phosphorus atoms position in z . As a consequence, it is possible to find a water molecule having a lower value of D than the one expected in that region. As shown in Fig. 3, the AQP region is not symmetric and there are higher values of D_{PORE} at negative distances, d , from the membrane centre than at positive ones. This is because the membrane protein is not symmetric and the diffusion around the protein is

asymmetric as a consequence.

Diffusion permeability and osmotic permeability

To compute the water permeability, both the diffusion (p_d) and osmotic permeability (p_f), we have calculated the rate at which molecules are able to cross the membrane (q_0 and k_0) and the diffusion of those molecules through the AQP (D_z). The results have been collected in Table 2, where we compare numerical and experimental data.

Table 2: Number of molecules per second (q_0 , multiplied by $(s^{-1}) 10^8$; diffusion permeability p_d , by $(cm^3/s) 10^{-14}$; osmotic permeability p_f , by $(cm^3/s) 10^{-14}$ ([*] via $p_f/p_d = 11.9$); number of molecules per second for an osmotic process k_0 , by $(s^{-1}) 10^9$; water diffusion inside the AQP D_z , by $(cm^2/s) 10^{-5}$ (**] via Eq. 2) and D_{PORE} , by $(cm^2/s) 10^{-5}$

Water model	q_0	p_d	p_f *	k_0 **	D_z **	D_{PORE}
TIP3P	4.0 (0.3)	1.20 (0.09)	14.2 (1.1)	4.85	0.190	0.10 (0.01)
TIP4P/2005	0.65 (0.2)	0.194 (0.07)	2.31 (0.8)	0.77	0.303	0.05 (0.02)
OPC	0.5 (0.1)	0.149 (0.04)	1.78 (0.4)	0.59	0.233	0.02 (0.02)
Exp.			5.43 ⁵⁰			0.04 ⁴⁵

Diffusion permeability (p_d) has been computed using Eq. 4, which is based on the number of water molecules that crossed the membrane through the membrane protein (q_0) and the volume of a single water molecule ($\nu_w = 2.989 \cdot 10^{-23} \text{ cm}^3$). From molecular dynamics simulations q_0 is a parameter that is easily accessible. For TIP3P $q_0 = 4.0 \cdot 10^8 \text{ s}^{-1}$ whereas for TIP4P/2005 ($q_0 = 0.65 \cdot 10^8 \text{ s}^{-1}$) and OPC ($q_0 = 0.5 \cdot 10^8 \text{ s}^{-1}$) the number of molecules per second is lower, by almost an order of magnitude. Therefore, we find 1) on the one hand an overestimation of the TIP3P diffusion permeability and 2) on the other hand a good performance of both TIP4P/2005 and OPC diffusion permeability (see Table 2).

The osmotic permeability p_f has been computed from the diffusion permeability using the ratio $p_f/p_d = N + 1 = 11.9$ proposed by Zhu *et al.*⁴⁶ for AQP1 and the values are reported in Table 2. The experimental data for p_f is $p_f = 5.43 \cdot 10^{-14} (\text{cm}^3/\text{s})$,⁵⁰ which is in excellent agreement with the TIP4P/2005 ($2.31 \cdot 10^{-14} \text{cm}^3/\text{s}$) and OPC ($1.78 \cdot 10^{-14} \text{cm}^3/\text{s}$)

values. The TIP3P value, $14.2 \cdot 10^{-14} \text{cm}^3/\text{s}$, is dramatically higher than the experimental value.

Having calculated the osmotic permeability, the rate of water crossing the AQP (q_0) can be calculated by applying Eq. 2 with a value of $z = 0.28 \text{ nm}$.⁴⁵ From the same Eq. 2, we calculated D_z for the different water models, obtaining $19.0 (\text{cm}^2/\text{s}) \cdot 10^{-7}$, $3.03 (\text{cm}^2/\text{s}) \cdot 10^{-7}$, and $2.33 (\text{cm}^2/\text{s}) \cdot 10^{-7}$ for TIP3P, TIP4P/2005 and OPC, respectively. TIP4P/2005 and OPC compare well with the experimental data, $4.0 (\text{cm}^2/\text{s}) \cdot 10^{-7}$.⁴⁵ However, TIP3P shows a value higher with respect to the experimental one than the other water models.

It is worth nothing that D_z could be compared to D_{PORE} using Eq. 1 as $dim = 1$. This fact allows us to test the consistency of our diffusion results, since D_{PORE} is calculated via Eq. 1 and D_z is computed via an independent method based on the number of water molecules that crossed the membrane through AQP (q_0) and its ratio with respect to the water permeability. As it can be observed, the results for water diffusion inside the AQP are essentially identical independent of the method used to compute it, either using Eq. 1 on the AQP region or applying Eq. 2.

In summary, our results provide compelling evidence that the TIP3P water model shows a higher diffusion rate than the other water models studied. Focusing on the diffusion through the AQP protein using two independent methods, we demonstrate that there is an overestimation of the diffusion, resulting in overestimated values of water permeability for TIP3P. However, for TIP4P/2005 and OPC, which have bulk diffusion values close to the experimental one, their calculated values of water permeability are comparable to the experimental value. This implies that TIP4P/2005 and OPC are capable of producing reliable estimates of water diffusion through the AQP1 channel.

Conclusion

In this work, water diffusion and permeability have been studied using molecular dynamics for three systems, consisting of AQP1 embedded in a POPC lipid membrane and three water models, TIP3P, TIP4P/2005 and OPC. TIP3P is the standard water model used for CHARMM36m, whereas TIP4P/2005 and OPC are water models not frequently used in biomolecular simulations but known to better reproduce bulk water properties.^{26,32} Our main purpose was to compare among the behaviour of different water models and shed light on AQP1 water permeability. This enabled us to obtain reliable results for the molecular mechanism of water diffusion as well as both diffusion and permeability values, near the membrane and through the AQP1. First of all, the well-known molecular mechanism of water transport through AQP1 has been tested for the three models, giving similar and excellent results. All of them show a specific orientation of water molecules inside the AQP1 as demonstrated in Ref.¹¹ Hence, using any of these water models, the water-protein interaction is reliable and AQP1 keeps its high-selectivity transport of water across the membrane.

The obvious difference among water models can be detected in the transport properties. Diffusion inside the protein has been computed using two methods, one based on the mean square displacement considering the geometry of the channel and another one from the water permeability, giving consistent results for the three models. TIP3P has a diffusion constant twice that of the experimental value, whereas TIP4P/2005 and OPC produce values remarkably close to experiment. The overestimation of TIP3P is consistent in the whole process of water transport across the membrane. The most relevant region is inside the membrane protein, *i.e.* the AQP region, where the TIP3P diffusion is 6, 9 and 4.5 times higher than TIP4P/2005, OPC and experimental data, respectively. It is worth noting that the ratios of TIP3P/TIP4P/2005 and TIP3P/OPC increase when moving from bulk to the interfacial region to the AQP region. Therefore, the difference between the models seems to be more pronounced within the nanopore environment.

Focusing on water permeability, we have computed the number of water molecules able to cross the membrane through the AQP1, q_0 . By means of this parameter we calculated the diffusion permeability, which allowed us to obtain the value of osmotic permeability. As in the diffusion case, TIP3P gives a diffusion permeability between 6 and 8 times higher than TIP4P/2005 and OPC, respectively.

The overestimation of TIP3P is observed also in the calculation of the osmotic permeability (being almost 3 times higher than the experimental counterpart) and in the water diffusion inside the AQP1 (being 5 times higher than the experimental counterpart). However the calculated values obtained with the OPC and TIP4P/2005 water models are in much better agreement with the experiments. It is difficult to compute the osmotic permeability in experiments and there are several values of p_f . However, in this work reliable values of water diffusion and water permeability are reported, which demonstrate the clear differences between the behaviour of TIP3P and the results of TIP4P/2005 and OPC. We believe that this observation can be relevant not only for the AQP channel but also for numerical studies of transport properties of water and ions within nanopores and ion channels.

Appendix A

As shown in the following Fig. 4 for TIP4P/2005, this charge distribution induces a negative value of μ_z (black line), while the other dipole moment components (green and red lines) are practically zero.

As shown in the figure, the baseline of μ_z is negative. This is caused by the system size, which is not large enough to remove finite size effects on the dipole moment. Hence, the total dipole moment (in blue) has a positive baseline and two maxima at the water-membrane interface, due to the z component contribution.

The other water models show a similar behaviour both for the density profiles and the dipole moment (data not shown). However, finite size effects on μ are not relevant for the

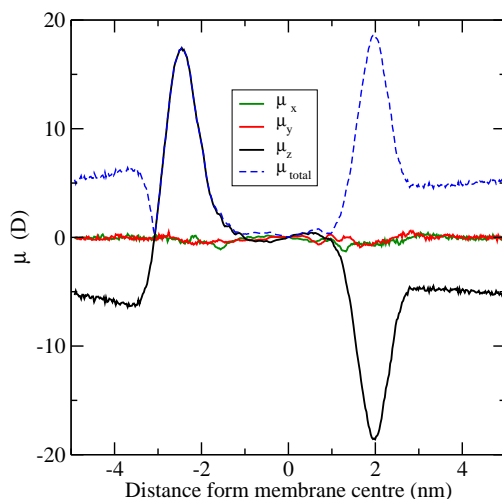


Figure 4: Average dipole moment for TIP4P/2005 along the z axis. The green solid line is the x component of dipole moment, in red the y component, in black the z component and in blue the total dipole moment. The total dipole moment is the dashed blue line.

water molecules inside the channel and their orientation reveals two clearly distinguishable regions, one positive and the other negative, as in Fig. 1 from the main text.

Acknowledgement

M.A.G. thanks for the support by Ayuda Juan de la Cierva-Incorporación (IJCI-2016-27497) from Ministerio de Ciencia, innovación y universidades (Spain) and HPC-Europa3 for funding the visit to Prof. Sansom's laboratory. M.S.P. Sansom acknowledges the following fundings: BBSRC BB/N000145/1 EPSRC EP/R004722/1 and EP/V010948/1, and C. Valeriani acknowledges fundings from MINECO PID2019-105343GB-I00.

Supporting Information Available

References

- (1) Beitz, E., Ed. *Aquaporins*; Handbook of Experimental Pharmacology; Springer Berlin Heidelberg: Berlin, Heidelberg, 2009; Vol. 190.

- (2) Yang, B., Ed. *Aquaporins*; Advances in Experimental Medicine and Biology; Springer Netherlands: Dordrecht, 2017; Vol. 969.
- (3) Castle, N. A. Aquaporins as targets for drug discovery. *Drug Discov. Today* **2005**, *10*, 485–493.
- (4) Day, R. E.; Kitchen, P.; Owen, D. S.; Bland, C.; Marshall, L.; Conner, A. C.; Bill, R. M.; Conner, M. T. Human aquaporins: Regulators of transcellular water flow. *Biochim. Biophys. Acta - Gen. Subj.* **2014**, *1840*, 1492–1506.
- (5) Kruse, E.; Uehlein, N.; Kaldenhoff, R. The aquaporins. *Genome Biol.* **2006**, *7*, 206.
- (6) Agre, P.; Kozono, D. Aquaporin water channels: Molecular mechanisms for human diseases. *FEBS Lett.* **2003**, *555*, 72–78.
- (7) Preston, G. M.; Carroll, T. P.; Guggino, W. B.; Agre, P. Appearance of water channels in *Xenopus* oocytes expressing red cell CHIP28 protein. *Science* **1992**, *256*, 385–7.
- (8) Walz, T.; Hirai, T.; Murata, K.; Heymann, J. B.; Mitsuoka, K.; Fujiyoshi, Y.; Smith, B.; Agre, P.; Engel, A. The Three-Dimensional Structure of Recombinant. *Nature* **1997**, *101*, 624–.
- (9) Chen, H.; Wu, Y.; Voth, G. A. Origins of Proton Transport Behavior from Selectivity Domain Mutations of the Aquaporin-1 Channel. *Biophys. J.* **2006**, *90*, L73–L75.
- (10) Kosinska Eriksson, U.; Fischer, G.; Friemann, R.; Enkavi, G.; Tajkhorshid, E.; Neutze, R. Subangstrom Resolution X-Ray Structure Details Aquaporin-Water Interactions. *Science (80-.)*. **2013**, *340*, 1346–1349.
- (11) Tajkhorshid, E.; Nollert, P.; Jensen, M. Ø.; Miercke, L. J. W.; O’Connell, J.; Stroud, R. M.; Schulten, K. Control of the Selectivity of the Aquaporin Water Channel Family by Global Orientational Tuning. *Science (80-.)*. **2002**, *296*, 525–530.

- (12) de Groot, B. L.; Engel, A.; Grubmüller, H. A refined structure of human aquaporin-1. *FEBS Lett.* **2001**, *504*, 206–211.
- (13) Law, R. J.; Sansom, M. S. P. Homology modelling and molecular dynamics simulations: comparative studies of human aquaporin-1. *Eur. Biophys. J.* **2004**, *33*, 477–489.
- (14) Ariz-Extreme, I.; Hub, J. S. Potential of Mean Force Calculations of Solute Permeation Across UT-B and AQP1: A Comparison between Molecular Dynamics and 3D-RISM. *J. Phys. Chem. B* **2017**, *121*, 1506–1519.
- (15) Decker, K.; Page, M.; Boyd, A.; MacAllister, I.; Ginsberg, M.; Aksimentiev, A. Selective Permeability of Truncated Aquaporin 1 in Silico. *ACS Biomater. Sci. Eng.* **2017**, *3*, 342–348.
- (16) de Groot, B. L.; Grubmüller, H.; Guggino, W. B.; Agre, P.; O’Connell, J.; Stroud, R. M.; Schulten, K.; Grubmüller, H. Water permeation across biological membranes: Mechanism and dynamics of aquaporin-1 and GlpF. *Science (80-.)*. **2001**, *294*, 2353–2357.
- (17) de Groot, B. L.; Frigato, T.; Helms, V.; Grubmüller, H. The mechanism of proton exclusion in the aquaporin-1 water channel. *J. Mol. Biol.* **2003**, *333*, 279–293.
- (18) Hashido, M.; Ikeguchi, M.; Kidera, A. Comparative simulations of aquaporin family: AQP1, AQPZ, AQP0 and GlpF. *FEBS Lett.* **2005**, *579*, 5549–5552.
- (19) Hub, J. S.; de Groot, B. L. Does CO₂ Permeate through Aquaporin-1? *Biophys. J.* **2006**, *91*, 842–848.
- (20) Hub, J. S.; Aponte-Santamaría, C.; Grubmüller, H.; de Groot, B. L. Voltage-Regulated Water Flux through Aquaporin Channels In Silico. *Biophys. J.* **2010**, *99*, L97–L99.
- (21) Mamonov, A. B.; Coalson, R. D.; Zeidel, M. L.; Mathai, J. C. Water and deuterium oxide permeability through aquaporin 1: MD predictions and experimental verification. *J. Gen. Physiol.* **2007**, *130*, 111–116.

- (22) Jensen, M. Ø.; Tajkhorshid, E.; Schulten, K. Electrostatic Tuning of Permeation and Selectivity in Aquaporin Water Channels. *Biophys. J.* **2003**, *85*, 2884–2899.
- (23) Zhu, F. Q.; Tajkhorshid, E.; Schulten, K. Pressure-induced water transport in membrane channels studied by molecular dynamics. *Biophys. J.* **2002**, *83*, 154–160.
- (24) Lee, S. C.; Khalid, S.; Pollock, N. L.; Knowles, T. J.; Edler, K.; Rothnie, A. J.; Thomas, O. R. T.; Dafforn, T. R. Encapsulated membrane proteins: A simplified system for molecular simulation. *Biochim. Biophys. Acta-Biomembranes* **2016**, *1858*, 2549–2557.
- (25) Ozu, M.; Alvarez, H. A.; McCarthy, A. N.; Grigera, J. R.; Chara, O. Molecular dynamics of water in the neighborhood of aquaporins. *Eur. Biophys. J.* **2013**, *42*, 223–239.
- (26) Vega, C.; Abascal, J. L. F. Simulating water with rigid non-polarizable models: a general perspective. *Physical Chemistry Chemical Physics* **2011**, *13*, 19663.
- (27) Onufriev, A. V.; Izadi, S. Water models for biomolecular simulations. *Wiley Interdisciplinary Reviews: Computational Molecular Science* **2018**, *8*, e1347.
- (28) Huang, J.; Rauscher, S.; Nawrocki, G.; Ran, T.; Feig, M.; de Groot, B. L.; Grubmüller, H.; MacKerell, A. D. CHARMM36m: an improved force field for folded and intrinsically disordered proteins. *Nat. Methods* **2017**, *14*, 71–73.
- (29) Best, R. B.; Mittal, J. Protein Simulations with an Optimized Water Model: Cooperative Helix Formation and Temperature-Induced Unfolded State Collapse. *J. Phys. Chem. B* **2010**, *114*, 14916–14923.
- (30) Abraham, M. J.; Murtola, T.; Schulz, R.; Páll, S.; Smith, J. C.; Hess, B.; Lindahl, E. GROMACS: High performance molecular simulations through multi-level parallelism from laptops to supercomputers. *SoftwareX* **2015**, *1-2*, 19–25.

- (31) Jorgensen, W. L. Quantum and statistical mechanical studies of liquids .10. Transferable intermolecular potential functions for water, alcohols, and ethers - Application to liquid water. *J. Am. Chem. Soc* **1981**, *103*, 335–340.
- (32) Izadi, S.; Anandakrishnan, R.; Onufriev, A. V. Building Water Models: A Different Approach. *The Journal of Physical Chemistry Letters* **2014**, *5*, 3863–3871.
- (33) Abascal, J. L. F.; Vega, C. A general purpose model for the condensed phases of water: TIP4P/2005. *J. Chem. Phys.* **2005**, *123*, 234505.
- (34) Bussi, G.; Donadio, D.; Parrinello, M. Canonical sampling through velocity rescaling. *J. Chem. Phys.* **2007**, *126*, 14101.
- (35) Parrinello, M.; Rahman, A. Polymorphic Transitions in Single Crystals: A New {M}olecular {D}ynamics Method. *J. Appl. Phys.* **1981**, *52*, 7182–7190.
- (36) Essmann, U.; Perera, L.; Berkowitz, M. L.; Darden, T.; Lee, H.; Pedersen, L. G. A smooth particle mesh Ewald method. *J. Chem. Phys.* **1995**, *103*, 8577–8593.
- (37) Róg, T.; Murzyn, K.; Pasenkiewicz-Gierula, M. The dynamics of water at the phospholipid bilayer surface: a molecular dynamics simulation study. *Chem. Phys. Lett.* **2002**, *352*, 323–327.
- (38) Bhide, S. Y.; Berkowitz, M. L. Structure and dynamics of water at the interface with phospholipid bilayers. *J. Chem. Phys.* **2005**, *123*, 224702.
- (39) Yamamoto, E.; Akimoto, T.; Hirano, Y.; Yasui, M.; Yasuoka, K. Supporting Information to “ Power-law trappings of water molecules on the lipid membrane surface induce the water retardation ”. *Phys. Rev. E - Stat. Nonlinear, Soft Matter Phys.* **2013**, *87*, 1–6.
- (40) Yang, J.; Calero, C.; Martí, J. Diffusion and spectroscopy of water and lipids in fully hydrated dimyristoylphosphatidylcholine bilayer membranes. *J. Chem. Phys.* **2014**, *140*.

- (41) Toppozini, L.; Roosen-Runge, F.; I. Bewley, R.; M. Dalglish, R.; Perring, T.; Seydel, T.; Glyde, H. R.; García Sakai, V.; Rheinstädter, M. C. Anomalous and anisotropic nanoscale diffusion of hydration water molecules in fluid lipid membranes. *Soft Matter* **2015**, *11*, 8354–8371.
- (42) Yamamoto, E.; Akimoto, T.; Yasui, M.; Yasuoka, K. Origin of subdiffusion of water molecules on cell membrane surfaces. *Sci. Rep.* **2015**, *4*, 4720.
- (43) Zaragoza, A.; Gonzalez, M. A.; Joly, L.; López-Montero, I.; Canales, M. A.; Benavides, A. L.; Valeriani, C. Molecular dynamics study of nanoconfined TIP4P/2005 water: how confinement and temperature affect diffusion and viscosity. *Phys. Chem. Chem. Phys.* **2019**, *21*, 13653–13667.
- (44) Berezhkovskii, A.; Hummer, G. Single-file transport of water molecules through a carbon nanotube. *Phys. Rev. Lett.* **2002**, *89*, 064503/1–064503/4.
- (45) Horner, A.; Zocher, F.; Preiner, J.; Ollinger, N.; Siligan, C.; Akimov, S. A.; Pohl, P. The mobility of single-file water molecules is governed by the number of H-bonds they may form with channel-lining residues. *Sci. Adv.* **2015**, *1*, e1400083.
- (46) Zhu, F. Q.; Tajkhorshid, E.; Schulten, K. Theory and simulation of water permeation in aquaporin-1. *Biophys. J.* **2004**, *86*, 50–57.
- (47) Finkelstein, A. *Water movement through lipid bilayers, pores, and plasma membranes: theory and reality*; Distinguished lecture series of the Society of General Physiologists; Wiley & Sons: New York, 1987; p 228.
- (48) Mathai, J. C.; Mori, S.; Smith, B. L.; Preston, G. M.; Mohandas, N.; Collins, M.; van Zijl, P. C. M.; Zeidel, M. L.; Agre, P. Functional Analysis of Aquaporin-1 Deficient Red Cells. *J. Biol. Chem.* **1996**, *271*, 1309–1313.

- (49) MacKerell, A. D.; Bashford, D.; Bellott, M.; Dunbrack, R. L.; Evanseck, J. D.; Field, M. J.; Fischer, S.; Gao, J.; Guo, H.; Ha, S. et al. All-atom empirical potential for molecular modeling and dynamics studies of proteins. *J. Phys. Chem. B* **1998**, *102*, 3586–3616.
- (50) Walz, T.; Smith, B. L.; Zeidel, M. L.; Engel, A.; Agre, P. Biologically active two-dimensional crystals of aquaporin CHIP. *J. Biol. Chem.* **1994**, *269*, 1583–1586.

Graphical TOC Entry

Some journals require a graphical entry for the Table of Contents. This should be laid out “print ready” so that the sizing of the text is correct.

Inside the tocentry environment, the font used is Helvetica 8 pt, as required by *Journal of the American Chemical Society*.

The surrounding frame is 9 cm by 3.5 cm, which is the maximum permitted for *Journal of the American Chemical Society* graphical table of content entries. The box will not resize if the content is too big: instead it will overflow the edge of the box.

This box and the associated title will always be printed on a separate page at the end of the document.